

VU Research Portal

Unnested islands of period-doublings in an injected semiconductor laser

Wieczorek, S.; Krauskopf, B.; Lenstra, D.

published in

Physical Review E
2001

document version

Publisher's PDF, also known as Version of record

[Link to publication in VU Research Portal](#)

citation for published version (APA)

Wieczorek, S., Krauskopf, B., & Lenstra, D. (2001). Unnested islands of period-doublings in an injected semiconductor laser. *Physical Review E*, 64, 056204-1-8.

General rights

Copyright and moral rights for the publications made accessible in the public portal are retained by the authors and/or other copyright owners and it is a condition of accessing publications that users recognise and abide by the legal requirements associated with these rights.

- Users may download and print one copy of any publication from the public portal for the purpose of private study or research.
- You may not further distribute the material or use it for any profit-making activity or commercial gain
- You may freely distribute the URL identifying the publication in the public portal ?

Take down policy

If you believe that this document breaches copyright please contact us providing details, and we will remove access to the work immediately and investigate your claim.

E-mail address:

vuresearchportal.ub@vu.nl

Unnested islands of period doublings in an injected semiconductor laser

Sebastian Wieczorek,^{1,*} Bernd Krauskopf,² and Daan Lenstra¹

¹*Faculty of Sciences, Vrije Universiteit, De Boelelaan 1081, 1081 HV Amsterdam, The Netherlands*

²*Department of Engineering Mathematics, University of Bristol, Bristol BS8 1TR, United Kingdom*

(Received 17 April 2001; published 12 October 2001)

We present a theoretical study of unnested period-doubling islands in three-dimensional rate equations modeling a semiconductor laser subject to external optical injection. In this phenomenon successive curves of period doublings are not arranged in nicely nested islands, but intersect each other. This overall structure is globally organized by several codimension-2 bifurcations. As a consequence, the chaotic region existing inside an unnested island of period doublings can be entered not only via a period-doubling cascade but also via the breakup of a torus, and even via the sudden appearance of a chaotic attractor. In order to fully understand these different chaotic transitions we reveal underlying global bifurcations and we show how they are connected to codimension-2 bifurcation points. Unnested islands of period doublings appear to be generic and hence must be expected in a large class of dynamical systems.

DOI: 10.1103/PhysRevE.64.056204

PACS number(s): 05.45.-a, 02.30.Oz, 42.55.Px

I. INTRODUCTION

A semiconductor laser on its own exhibits only simple dynamics: typically any perturbation damps out in an oscillatory fashion with the relaxation oscillation frequency ω_R [1]. However, low facet reflectivities (of around only 30%) and the self-phase modulation effect (the refractive index in the semiconductor material depends on the population inversion) make this type of laser very sensitive to external influences, such as optical injection or optical feedback. It is well known that in their presence a semiconductor laser may become very unstable and produce amazingly rich and complex nonlinear dynamics [2,6]. A semiconductor laser with optical injection constitutes the simplest semiconductor laser system that produces dynamics ranging from periodic output to several types of chaotic behavior [3–5]. Although most applications take advantage of stable operation, their chaotic output makes optically injected semiconductor lasers very interesting from several points of view. First, chaotic dynamics has recently received a lot of interest due to its possible use for dynamics based computation [7] and chaotic communication [8–11,14]. Second, studying the complex dynamics of optically injected semiconductor lasers appears to be an important step on the way to understanding these devices. Furthermore, the theoretical model is simple enough to allow for bifurcation analysis and, most importantly, it describes experimental observations surprisingly well [3,15]. This provides a rare opportunity for studying chaotic transitions in a system that is experimentally accessible.

There exist several ways in which a dynamical system can become chaotic, of which the period-doubling route to chaos is the best known; see, e.g., [16,17]. In a two-dimensional parameter space one finds that the curves of period doubling locally accumulate according to the Feigenbaum constant, finally leading to a region of chaotic dynamics. If these curves are all closed curves that are nicely nested then the

region of chaos can be reached and left only by period doublings; see Fig. 2 below.

In this paper we show that the curves of period doublings need not be nested, but can intersect; an example is shown in Fig. 3(a) below. This is possible only if the period-doubling curves interact with and are linked to other bifurcations, as is illustrated in Fig. 3(b) below. This complicated web of bifurcations will be studied in detail. It is crucial how certain codimension-2 bifurcations organize the dynamics; see [18] for a study of an optically pumped three-level laser model. Our overall result is that the chaotic region in an unnested island of period doublings can be reached in other ways, most importantly via sudden chaotic transitions such as a boundary crisis and saddle node of periodic orbit bifurcation taking place on a chaotic attractor [19].

Although the first theoretical studies of sudden changes in chaotic dynamics started in the early 1980's [20–24] the problem is still of great interest, also in laser systems [19,25–30], and not completely understood yet, especially in the case that periodic dynamics suddenly replaces chaos [31,32]. In order to fully understand discontinuous changes of chaotic attractors we compute stable and unstable manifolds of appropriate saddle orbits. To complete the picture, we identify bifurcation curves in the two-dimensional parameter plane [the (K, ω) plane introduced in Sec. III] along which these sudden chaotic transitions occur. While our results are important for understanding complicated dynamics in the laser systems at hand, the phenomenon described here will also appear in other dynamical systems.

We want to make clear that by a sudden transition we mean a sudden or discontinuous change in the nature of the attractor when parameters are changed. However, in a real system nothing happens instantly, so that one needs to let transients die down in order to see the new attractor. Nevertheless, the changes described here are sudden compared to situations where an attractor changes continuously with the parameters during the bifurcation (as is the case, for example, for a periodic orbit disappearing in a Hopf bifurcation).

*Corresponding author. Electronic address: sebek@nat.vu.nl

The paper is organized as follows. In Sec. II we introduce and discuss the rate equation model of a semiconductor laser with optical injection. Unnested period doublings and the resulting discontinuous chaotic transitions are presented in Secs. III and IV. In Sec. V we explore global bifurcations underlying these sudden chaotic transitions and reveal their origin in parameter space in certain codimension-2 bifurcations. Conclusions are drawn in Sec. VI.

II. THE RATE EQUATION MODEL

A single-mode diode laser with monochromatic optical injection can be modeled by *three-dimensional* rate equations for the slowly varying complex electric field $E = E_x + iE_y$ and the normalized inversion n inside the laser [3]:

$$\begin{aligned} \dot{E} &= K + \left(\frac{1}{2}(1 + i\alpha)n - i\omega \right) E, \\ \dot{n} &= -2\Gamma n - (1 + 2Bn)(|E|^2 - 1). \end{aligned} \quad (1)$$

Equations (1) are scaled for convenience; the connection between the scaled (dimensionless) quantities used here and experimental quantities is given in [3].

The most important parameters are the strength K of the field that is injected from an external source into the laser, and the detuning ω of its frequency from the frequency of the free-running laser. Both can easily be changed during an experiment and, therefore, are natural operational parameters. The quantities B and Γ , on the other hand, represent material properties of the laser and are fixed to the realistic values $B = 0.015$ and $\Gamma = 0.035$. The parameter α is called the linewidth enhancement factor, and it quantifies how much the refractive index, and hence the instantaneous laser resonance frequency, changes with the population inversion n [3]. Throughout this paper we focus on the case $\alpha = 2$ for definiteness, but similar results can be found throughout a range of realistic α values.

We look at Eqs. (1) from a dynamical systems point of view and study different kinds of dynamical behavior represented by different objects in the three-dimensional phase space, the (E, n) space. All these objects have a physical meaning and describe certain phenomena occurring in the laser. In order to translate a situation from the phase space to ‘‘real life’’ one needs to remember that Eqs. (1) are written in the reference frame of the injected field frequency. This means that an attracting stationary point corresponds to the laser operating at constant intensity, constant population inversion, and the frequency of the injected light: the laser locks to the injected field. A periodic orbit generally corresponds to an oscillatory exchange of the energy inside the laser between the population inversion and the electric field. A torus corresponds to beating between two oscillations, usually one associated with the detuning ω and the relaxation oscillation, which tend to synchronize as their coupling strength increases. A chaotic attractor corresponds to irregular and unpredictable laser output.

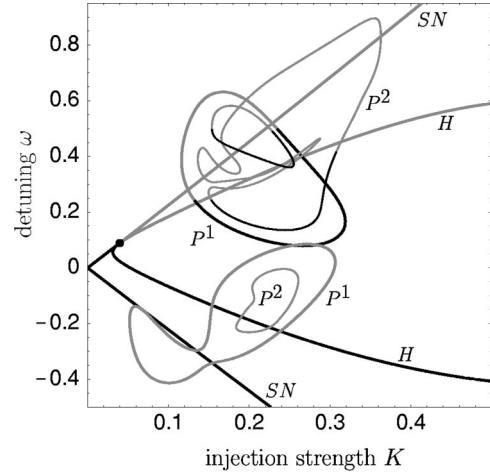


FIG. 1. The bifurcation diagram of Eqs. (1) in the (K, ω) plane. In this and all figures of the (K, ω) plane, ω is in multiples of ω_R while K is dimensionless.

III. THE BIFURCATION DIAGRAM

Transitions between different kinds of dynamics are bifurcations, and curves of different bifurcations divide the (K, ω) plane, the parameter space of Eqs. (1), into regions of different qualitative dynamics of the laser. We now study the bifurcation diagram which consists of bifurcation curves in the (K, ω) plane together with representative phase portraits. The bifurcation curves presented here were computed with the package AUTO [33]. Figure 1 shows the bifurcations of stationary points, namely, the saddle-node and Hopf bifurcation curves SN and H , and curves P^1 of (first) period doublings; see [3] for the full picture and its dependence on α . Note how the nested and unnested period-doubling islands from Figs. 2 and 3 are part of this bifurcation diagram. Supercritical bifurcations of stable objects are plotted in black and subcritical bifurcations of unstable objects in gray. The black part of SN forms the lower boundary of the laser’s locking range [the region in the (K, ω) plane where the laser locks to the external field], because along this curve a stable stationary point is created. This stationary point becomes unstable along the black part of the Hopf bifurcation curve H , which gives rise to an attracting periodic orbit. Physically, the relaxation oscillation is excited and the laser emits light with a periodically varying amplitude. The curve H forms

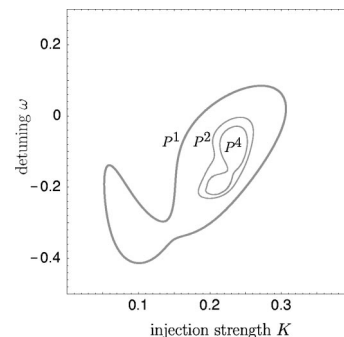


FIG. 2. Nested islands of period doublings.

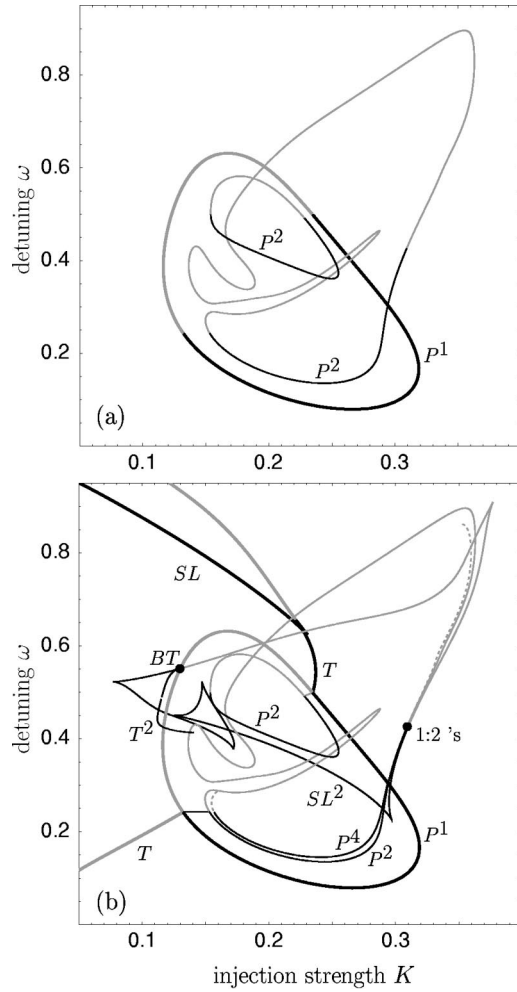


FIG. 3. Unnested islands of period doublings (a), and the complicated web of bifurcations involved (b).

the upper boundary of the locking range (where the phase is constant). Note that above H initially the phase is still bounded while it oscillates. The attracting periodic orbit originating from H may undergo further bifurcations, for example, period doubling along the black parts of the curves denoted P^1 . Note that the repelling periodic orbit created along the gray part of H doubles its period when the lowest, subcritical period doubling bubble P^1 is crossed.

The superscript of P^1 denotes that we are dealing with a period doubling of a ‘‘basic’’ periodic orbit, which can then undergo further period doublings as part of an infinite cascade of period doublings leading to chaos. Secondary period-doubling curves P^n , where $n=2,4,\dots$, accumulate at the rate of Feigenbaum’s universal constant [17,20]. In the simplest case, one would expect secondary period-doubling bubbles to accumulate inside the P^1 bubbles. An example of this is shown in Fig. 2 where all closed curves of period doublings are indeed nicely nested inside P^1 . The region of chaotic dynamics inside this bifurcation structure can be entered or exited only via a cascade of successive period doublings.

However, curves of successive period doublings need not be nested, and this is shown in Fig. 3(a) which shows the

other small P^1 bubble from Fig. 1. Notice that there are two closed curves of secondary period doubling P^2 : one lies strictly inside P^1 , but the other leaves the confines of P^1 . This is possible only if there are intricate interactions with other bifurcations, and this is shown in Fig. 3(b). Most importantly, there are torus (or Neimark-Sacker) and saddle-node bifurcations of periodic orbits (T and T^2 , SL and SL^2). They form an intricate web of bifurcation curves, which involves several codimension-2 bifurcations. First, there is a Bogdanov-Takens bifurcation for maps, also called a 1:1 resonance, denoted by BT in Fig. 3(b). At BT the saddle node of the curve SL^2 of periodic orbits changes from super- to subcritical and a torus curve T^2 emanates.

Furthermore, a torus bifurcation curve can end at a period-doubling curve at the codimension-2 point called a 1:2 resonance, which also changes the period doubling from super- to subcritical. There are two cases (see, e.g., [17]) depending on a normal form coefficient. The case in Fig. 3(b) is also called torus doubling because a period-doubled torus emerges. This gives the possibility for a cascade of 1:2 resonance points with short pieces of torus bifurcation curves connecting successive period doublings. Such a cascade appears at the point denoted by 1:2’s in Fig. 3(b), but here the 1:2 resonance points are extremely close together. This phenomenon is discussed in more detail in the Appendix.

Indeed it is the presence of these extra bifurcations that allows the curves of secondary period doublings to go outside P^1 . The parts of P^2 from Fig. 3 that go outside P^1 correspond to bifurcations of either an orbit that became unstable via a torus bifurcation or of one of the two extra orbits created in the saddle node of a periodic orbit bifurcation. In the next section we describe different transitions, while further discussion of the bifurcation diagram in Fig. 3(b) is the topic of Sec. V.

IV. TRANSITIONS TO CHAOS

The existence of an unnested period-doubling structure reveals an interesting question. Let us suppose that we change parameters and enter the P^1 bubble in Fig. 3 by crossing an infinite number of curves P^n , so that we end up with chaotic laser output. Then, since the period-doubling islands are unnested, we can choose to leave the chaotic region in Fig. 3 in such a way that no period-doubling curves are crossed. What is then the transition from the chaotic attractor to the periodic orbit known to exist outside P^1 ? Clearly the nature of the transition depends on the route chosen in parameter space. We illustrate this below by plotting the corresponding attractors of the Poincaré map defined by the plane $\{n=0\}$. Furthermore, we show time series and appropriate stable and unstable manifolds of saddle points in the Poincaré section. All phase portraits presented here were computed with DSTOOL [34], and the manifolds with the method of [35,36]. Throughout the paper, unstable manifolds W^u are in black and stable manifolds W^s are in gray.

A. Intermittent transition

In Fig. 4 we fix the injection strength to $K=0.26$ and increase the detuning ω ; see Fig. 3. The starting point is the

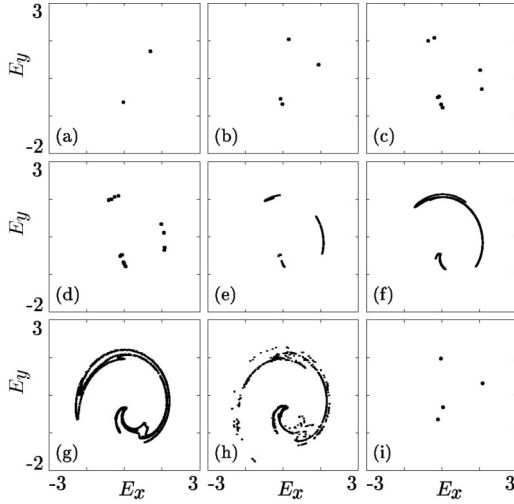


FIG. 4. Period-doubling route to chaos and sudden disappearance of chaos at a saddle-node bifurcation of a periodic orbit (intermittent transition). Shown are attractors in the Poincaré section $\{n=0\}$; $K=0.26$ while from (a) to (i) ω takes the values 0.05, 0.1, 0.15, 0.154, 0.16, 0.18, 0.25, 0.3105, and 0.311.

attracting periodic orbit [Fig. 4(a)] that exists for parameters below the P^1 bubble. When ω is increased the curve P^1 is encountered and the periodic orbit period doubles [Fig. 4(b)]. On increasing ω further, secondary period doublings are encountered [Figs. 4(c), 4(d), and 4(e)], resulting in the creation of a chaotic attractor [Figs. 4(f) and 4(g)]. From Fig. 3(b) we observe that increasing ω further will not result in inverse period doublings. In fact, the next bifurcation is the saddle node of periodic orbits SL^2 in which two period-2 orbits, one attracting and one a saddle, are created. As SL^2 is approached the chaotic attractor starts to anticipate the new attracting orbit that is about to appear [Fig. 4(h)]. As soon as SL^2 is crossed an attracting period-2 orbit appears and the chaotic attractor is suddenly gone [Fig. 4(i)].

In other words, we encountered a sudden transition from chaos to periodic oscillations. Note that there is no bistability or hysteresis present, so that there is a sudden appearance of chaos at the saddle-node bifurcation when ω is decreased. Due to the character of the time series just before the chaotic attractor is destroyed, shown in Fig. 5, this is often called an intermittent transition: the time series shows windows of periodic behavior interrupted by occasional chaotic bursts. Closer to the saddle-node bifurcation the bursts are less and less frequent and they disappear entirely after the periodic orbit is created. The sudden disappearance of chaos in a saddle-node bifurcation of periodic orbits is due to the

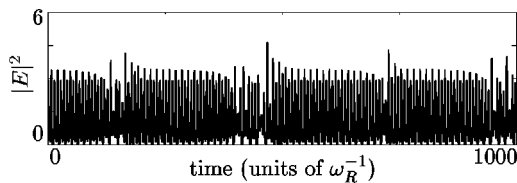


FIG. 5. Intermittent time series of the chaotic attractor from Fig. 4(h).

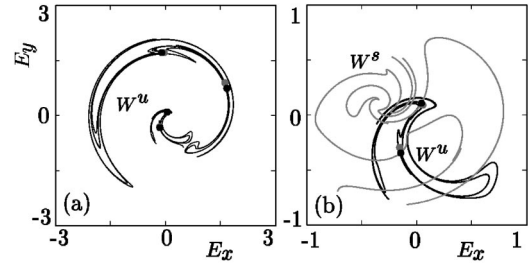


FIG. 6. The unstable manifold just after the saddle-node bifurcation for $\omega=0.311$ and $K=0.26$ (a) has the shape of the destroyed chaotic attractor from Fig. 4(h). Panel (b) shows the homoclinic tangle in the central region of panel (a).

saddle-node bifurcation taking place “on the chaotic attractor.” This is demonstrated in Fig. 6 by images of the stable and unstable manifolds of the saddle point very close to the saddle-node bifurcation. Notice that the unstable manifold W^u from Fig. 6(a) resembles the shape of the chaotic attractor before the bifurcation and that the stable and unstable manifolds (W^s and W^u) intersect in a homoclinic tangle [Fig. 6(b)]. With decreasing ω (going in the opposite direction) the two periodic orbits disappear and the complicated black manifold (technically, the center manifold) becomes the chaotic attractor.

Next we show that a chaotic attractor created in the breakup of a torus can also undergo an intermittent transition. To this end, in Fig. 7 we choose a path close to the point BT in Fig. 3(b). A torus grows in size [Fig. 7(b)] and then starts to break up [Figs. 7(c) and 7(d)] leading to a chaotic attractor [Fig. 7(e)]. This chaotic attractor suddenly disappears and we are left with an attracting periodic orbit [Fig. 7(f)]. As is shown in Fig. 8, the time series again displays intermittent chaotic bursts just before the bifurcation. Indeed, Fig. 9 shows that stable and unstable manifolds of the saddle intersect transversely in a homoclinic tangle just after the bifurcation, which is the hallmark of this bifurcation.

One may think that the intermittent transition is the only sudden transition in the unnested period-doubling structure. However, this is not the case as we show now.

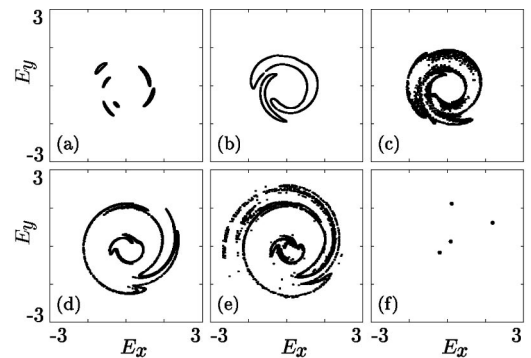


FIG. 7. Breakup of a torus and sudden disappearance of chaos at a saddle-node bifurcation of periodic orbits (intermittent transition); (a) and (b) $\omega=0.43$, $K=0.1139$, 0.1145 , and from (c) to (f) $\omega=0.42$, $K=0.12$, 0.145 , 0.166 , 0.167 .

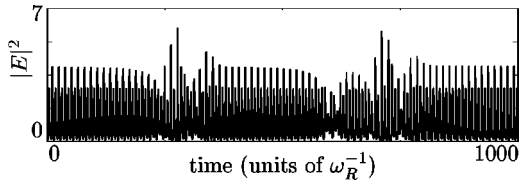


FIG. 8. Intermittent time series of the chaotic attractor from Fig. 7(e).

B. Boundary crisis

In Fig. 10 we fix $\omega = 0.46$ and increase K from 0.115, so that we are close to the point BT in Fig. 3. We find a bistability between a periodic orbit (gray dots) created on SL^2 and a torus [Fig. 10(a)], which then breaks up, giving rise to coexistence of a periodic orbit and a chaotic attractor [Fig. 10(b)]. Then, suddenly the chaotic attractor disappears [Fig. 10(b)]. To understand what is going on we plot in Fig. 11 the time series for parameters just after the chaotic attractor disappeared. It shows a very long chaotic transient, because we started the system close to where the chaotic attractor was. This behavior is characteristic of what is called a boundary crisis [23], where a chaotic attractor hits the boundary of its basin of attraction and disappears. To show that this is indeed what happens, Fig. 12 presents the stable and unstable manifolds of a saddle periodic orbit on the chaotic attractor. In Fig. 12(a) one (the short) branch of the stable manifold accumulates on the stable periodic orbit (gray dots) while the other branch accumulates on the chaotic attractor. (It is conjectured that a chaotic attractor is always the closure of some unstable manifold; see, for example, [13].) The stable manifold forms the basin boundary between the two coexisting attractors, the periodic orbit and the chaotic attractor. The system will settle down to one of these attractors depending on which side of the stable manifold the initial condition is chosen. As K is increased we observe a homoclinic tangency [Fig. 12(b)] giving rise to homoclinic tangle [Figs. 12(c) and 12(d)]. Once the stable and unstable manifolds intersect, the chaotic attractor and its basin boundary are destroyed. More concretely, all trajectories will eventually “leak” to the attracting periodic orbit [37]. This explains the disappearance of the chaotic attractor as well as the long chaotic transients.

Near the accumulation of 1:2 resonances in Fig. 3(b) one also finds a boundary crisis. This is shown in Fig. 13 where again a chaotic attractor (in black) coexists with an attracting

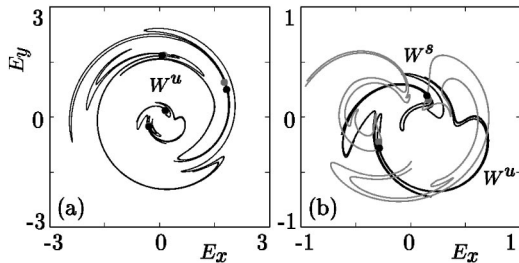


FIG. 9. The unstable manifold just after the saddle-node bifurcation for $K = 0.167$ and $\omega = 0.42$ (a) has the shape of the destroyed chaotic attractor from Fig. 7(e). Panel (b) shows the homoclinic tangle in the central region of panel (a).

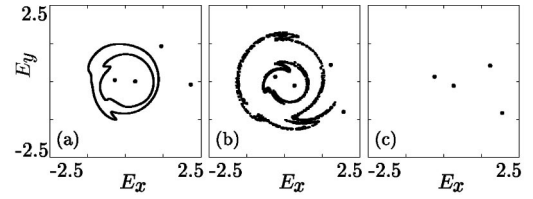


FIG. 10. A sudden destruction of the chaotic attractor (created in the breakup of a torus, and coexisting with the gray attracting periodic orbit) in a boundary crisis; from (a) to (c) $\omega = 0.46$ and K takes the values 0.115, 0.129, and 0.13.

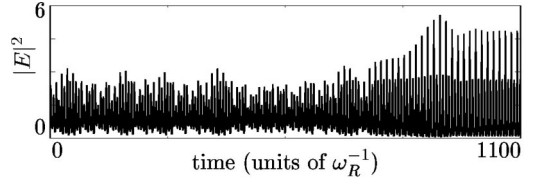


FIG. 11. Long chaotic transient before the trajectory settles down from near the former chaotic attractor to the attracting periodic orbit in Fig. 10(c) for $K = 0.13$ and $\omega = 0.46$.

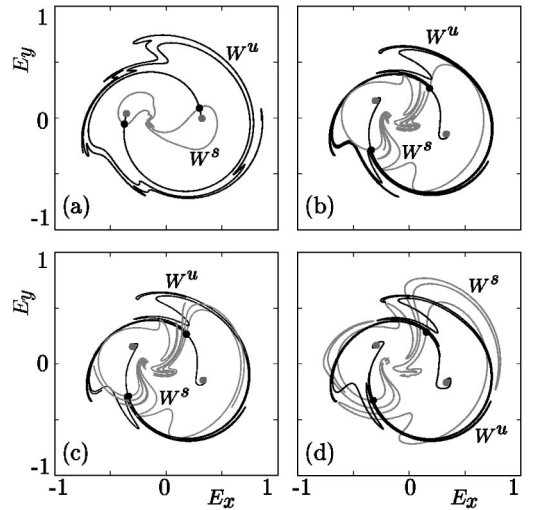


FIG. 12. Formation of homoclinic tangle of the black periodic orbit (originally on the chaotic attractor), demonstrating that Fig. 10 indeed shows a boundary crisis; $\omega = 0.46$ and from (a) to (d) K takes the values 0.115, 0.1297, 0.13, and 0.135.

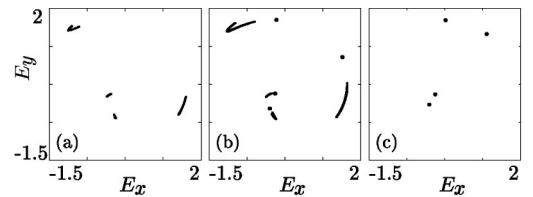


FIG. 13. A sudden destruction of the chaotic attractor (created in period doublings, and coexisting with the gray attracting periodic orbit) in a boundary crisis; from (a) to (c) $K = 0.2885$ and ω takes the values 0.253, 0.255, and 0.275.

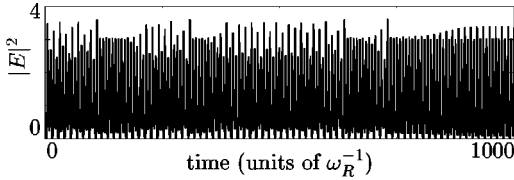


FIG. 14. Long chaotic transient before the trajectory settles down from near the former chaotic attractor to the attracting periodic orbit in Fig. 10(c) for $K=0.2885$ and $\omega=0.26$.

periodic orbit (gray dots) [Fig. 13(b)]. Notice that the chaotic attractor now has the typical, almost one-dimensional, shape of an attractor created in period doublings. Again, suddenly the chaotic attractor disappears [Fig. 13(c)], which goes along with long chaotic transients as is shown in Fig. 14. The manifolds in Fig. 15 show that we are indeed dealing with a boundary crisis. The homoclinic tangency [Fig. 15(b)] between the stable and unstable manifolds of the saddle orbit leads to the destruction of this attractor. Again, all trajectories will eventually go to the attracting periodic orbit (gray dots).

V. THE ROLE OF GLOBAL BIFURCATIONS

In the previous section we demonstrated that the chaotic region in the period-doubling bubble under consideration can be entered and exited via different transitions. In particular, we found homoclinic tangencies corresponding to boundary crisis. All this information is put together in schematic form in Fig. 16; compare Fig. 3(b). Different regions are numbered for reference. The overall structure is the following. The saddle node of the periodic orbit curve SL^2 has two cusps. From the point BT where the torus bifurcation curve T^2 touches and ends at SL^2 , two curves of homoclinic tangencies emerge (dashed curves), which bound a region of homoclinic tangle. It is known from bifurcation theory [17] that the point BT gives rise to a wedge with homoclinic tangle, whose boundaries are given by homoclinic tangencies. We found that the lower of these curves of homoclinic tangency connects to the curve SL^2 at a point H . At H the stable and center manifolds of the saddle node are tangent. This defines the left boundary of the left part of SL^2 giving rise to an intermittent transition.

On the right hand side and starting from SL^2 there are infinitely many period-doubling curves connected by short pieces of torus bifurcation curves via 1:2 resonance points. A 1:2 resonance point can have two cases of unfolding [17]

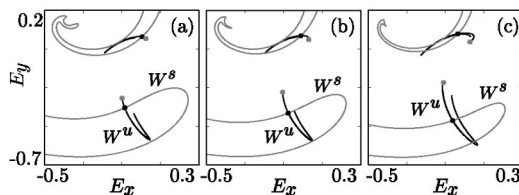


FIG. 15. Formation of homoclinic tangle of the black periodic orbit (originally on the chaotic attractor), demonstrating that Fig. 13 indeed shows a boundary crisis; $K=0.2885$ and from (a) to (c) ω takes the values 0.255, 0.26, and 0.275.

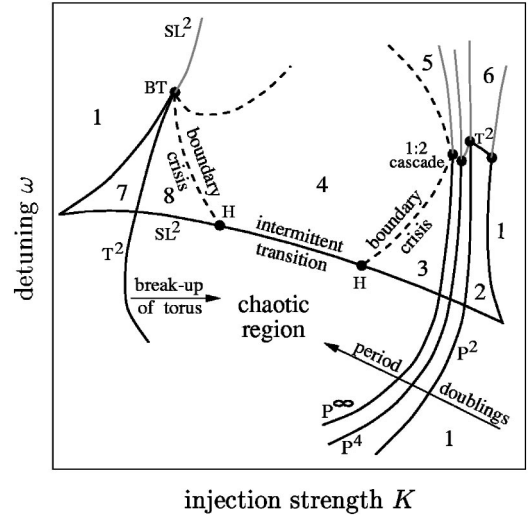


FIG. 16. Sketch of the structure of the unnnested period doublings from Fig. 3(b). The homoclinic tangency along the left curve of boundary crisis is shown in Fig. 12(b) and the homoclinic tangency along the right curve of boundary crisis is shown in Fig. 15(b). See Fig. 17 for sketches of phase portraits in the numbered regions.

depending on the sign of a certain normal form coefficient, but in both there is a change in the period doubling from super- to subcritical. Apparently, in our case there is a negative normal form coefficient (see [17], Sec. 9.5). Although the unfolding for the two-dimensional vector field normal form is known, the complete bifurcation picture in a three-dimensional vector field remains unknown. The accumulation of 1:2 resonances that we deal with here makes the situation even more complex, and a detailed study of this problem is beyond the scope of this paper. However, we present in the Appendix a partial unfolding justifying the existence of the curves sketched in Fig. 16. In particular, we found that there is a curve of homoclinic tangency emanating from the accumulation point of the 1:2 cascade on the right in Fig. 16, which also connects to the curve SL^2 . This defines the right boundary point H of the region where SL^2 gives rise to an intermittent transition.

These results were obtained by carefully computing stable and unstable manifolds in the respective parameter regions. Furthermore, we could identify the intersection points H by their property that the stable and center manifolds of the saddle node are tangent. An extra difficulty is that the Poincaré map is not globally defined, but only locally in certain regions of the section (for example, close to intersections with attracting periodic orbits). This causes problems in computing branches of stable and unstable manifolds. In this respect the injected laser studied here differs from periodically driven systems, where a Poincaré map is defined globally as a stroboscopic map; see, e.g. [12], p. 13.

VI. CONCLUSIONS

Using the example of the injected semiconductor laser we showed that period-doubling bifurcation curves do not always accumulate inside each other but often form unnnested

islands. In consequence, the region of chaos inside these islands can be reached in several different ways depending on the chosen route in the parameter plane. We paid particular attention to transitions where chaotic dynamics suddenly disappear. Concretely, we identified a saddle-node bifurcation of periodic orbits on a chaotic attractor (intermittent transition) and a boundary crisis.

Furthermore, we showed how these transitions are embedded in a consistent bifurcation diagram of unnested period doublings. The main ingredients are homoclinic tangencies emerging from codimension-2 bifurcations, namely, from a Bogdanov-Takens bifurcation of maps, and a 1:2 resonance cascade. This latter phenomenon is still not understood in detail, although we presented a partial conjectural unfolding.

Preliminary explorations show that the sudden changes in the output of the laser are accessible experimentally. This work is in progress and will be reported elsewhere.

ACKNOWLEDGMENTS

We thank Tom Simpson and Gautam Vemuri for stimulating discussions. This research was supported by the Foundation for Fundamental Research on Matter (FOM), which is financially supported by the Netherlands Organization for Scientific Research (NWO). B.K. acknowledges support by the British Council and NWO under the U.K.-Dutch Joint Scientific Research Programme.

APPENDIX: THE DYNAMICS NEAR A CASCADE OF 1:2 RESONANCES

We sketch here briefly the dynamics near the cascade of 1:2 resonance points that appears on the right of Fig. 16. An image of such a cascade, involving only the period-doubling and torus bifurcation curves can be found in [17], Sec. 9.6, but the general unfolding of this codimension-2 bifurcation phenomenon is still unknown. It is known, however, that the individual 1:2 resonance points involved in the cascade are starting points for curves of homoclinic tangencies that bound regions with homoclinic tangle; see, for example, [17].

We have investigated the 1:2 resonance cascade in the laser system at hand, and this resulted in the bifurcation structure shown in Fig. 17. The regions of different phase portraits are numbered just as in Fig. 16, and sketches of the respective phase portraits of a suitable Poincaré map are shown. There are infinitely many period-doubling curves connected by short pieces of torus bifurcation curves via 1:2 resonance points. At each such 1:2 resonance the period doubling changes from super- to subcritical and a curve of torus bifurcation of a doubled torus appears.

To describe this structure we start to the right of the curve SL^2 and explain what happens when the parameters are changed in a loop around the 1:2 resonance cascade. Phase portrait 1 shows a single attractor, but note that points hop from left to right and from top to bottom under the Poincaré map, which has two negative eigenvalues. Crossing SL^2 results in the creation of an attracting and a saddle-type period-2 orbit in phase portrait 2. In other words, we have

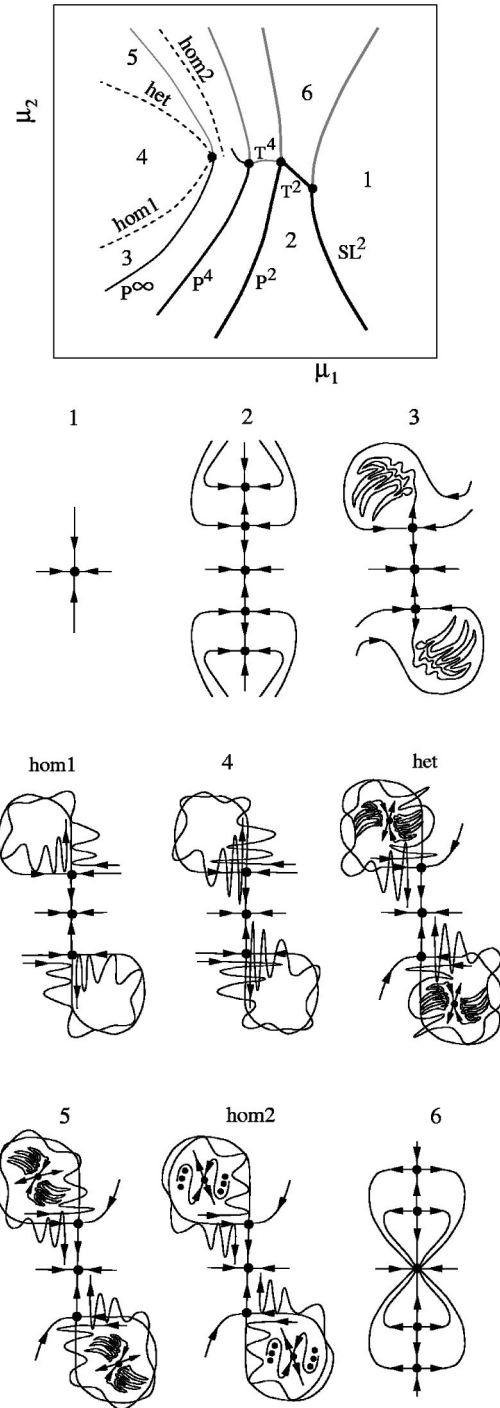


FIG. 17. A conjectural partial unfolding (in two parameters μ_1 and μ_2) of a 1:2 resonance cascade; compare Fig. 16. The heteroclinic tangency along “het” is shown in Fig. 18(b).

bistability where the boundary between the two basins of attraction is formed by the stable manifold of the saddle-type period-2 orbit. The period-2 attractor then undergoes successive period doublings, when the supercritical period-doubling curves P^2 up to P^∞ are crossed, leading finally to a bistability between the original period-1 orbit and a chaotic attractor in phase portrait 3. We found that this chaotic attractor is destroyed in a boundary crisis along the curve hom1; the numerical evidence of this homoclinic bifurcation

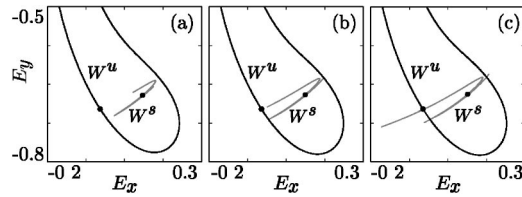


FIG. 18. Numerical evidence for the heteroclinic tangency sketched in Fig. 17; $\omega=0.56$ and K takes the values 0.3293, 0.329, and 0.3288 from (a) to (c).

was already presented in Fig. 15. The resulting phase portrait 4 then only has the original period-1 orbit as an attractor, but it also features homoclinic tangle between the stable and unstable manifolds of the period-2 saddle-type orbit.

As we follow the parameter further around the top of the 1:2 resonance cascade, we encounter the heteroclinic bifurcation curve leading to a chaotic repeller in phase portrait 5. A numerical picture of this heteroclinic bifurcation appears in Fig. 18. The chaotic repeller has initially a fractal-like boundary, which becomes more regular in the further homoclinic tangency hom2 (it is then formed by the unstable

manifold of the period-2 point). The chaotic repeller then period-undoubles when the subcritical period-doubling curves P^∞ down to P^2 are crossed. This finally results in phase portrait 6 where the original period-1 orbit is still the only attractor. In the subcritical saddle-node bifurcation of periodic orbits, SL^2 , the two period-2 orbits disappear. This brings the dynamics back to where we started in phase portrait 1.

This loop around the 1:2 resonance cascade is a consistent bifurcation scenario. It is sufficient to explain the existence of the curve of boundary crisis that appeared in Fig. 16 in the laser system we studied. Our results are backed by a thorough numerical investigation, during which we computed bifurcation curves and many stable and unstable manifolds. This led us to conjecture that Fig. 17 constitutes a partial unfolding of a 1:2 resonance cascade in the general situation.

On the other hand, as was mentioned earlier, we did not account for all homoclinic bifurcations that are known to exist near the individual 1:2 resonance points. Consequently, the general unfolding will be more complicated than sketched here, and finding it remains an interesting topic for future research.

- [1] G.H.M. van Tartwijk, and D. Lenstra, *Quantum Semiclass. Opt.* **7**, 87 (1995).
- [2] J. Sacher, D. Baums, P. Panknin, W. Elsässer, and E.O. Göbel, *Phys. Rev. A* **45**, 1893 (1992).
- [3] S.M. Wieczorek, B. Krauskopf, and D. Lenstra, *Opt. Commun.* **172**, 279 (1999).
- [4] S.M. Wieczorek, B. Krauskopf, and D. Lenstra, *Opt. Commun.* **183**, 215 (2000).
- [5] B. Krauskopf, S. Wieczorek, and D. Lenstra, *Appl. Phys. Lett.* **77**, 1611 (2000).
- [6] *Fundamental Issues of Nonlinear Laser Dynamics: Concepts, Mathematics, Physics, and Applications*, edited by B. Krauskopf and D. Lenstra, AIP Conf. Proc. No. 548 (AIP, Melville, NY, 2000).
- [7] S. Sinha, and W.L. Ditto, *Phys. Rev. Lett.* **81**, 2156 (1998).
- [8] C.R. Mirasso, P. Colet, and P. Garcia-Fernández, *IEEE Photonics Technol. Lett.* **8**, 299 (1996).
- [9] C.R. Mirasso, in *Fundamental Issues of Nonlinear Laser Dynamics: Concepts, Mathematics, Physics, and Applications* (Ref. [6]), pp. 112–127.
- [10] G.D. VanWiggeren and R. Roy, *Science* **279**, 1198 (1997).
- [11] R. Roy, in *Fundamental Issues of Nonlinear Laser Dynamics: Concepts, Mathematics, Physics, and Applications* (Ref. [6]), pp. 260–278.
- [12] B. Krauskopf, in *Fundamental Issues of Nonlinear Laser Dynamics: Concepts, Mathematics, Physics, and Applications* (Ref. [6]), pp. 1–30.
- [13] H.W. Broer and B. Krauskopf, in *Fundamental Issues of Nonlinear Laser Dynamics: Concepts, Mathematics, Physics, and Applications* (Ref. [6]), pp. 31–53.
- [14] H.F. Chen and J.M. Liu, *IEEE J. Quantum Electron.* **36**, 27 (2000).
- [15] T.B. Simpson, J.M. Liu, K.F. Huang, and K. Tai, *Quantum Semiclass. Opt.* **9**, 765 (1997).
- [16] E. Ott, *Chaos in Dynamical Systems* (Cambridge University Press, Cambridge, 1993).
- [17] Yu.A. Kuznetsov, *Elements of Applied Bifurcation Theory*, Vol. 112 of Applied Mathematical Sciences Series (Springer-Verlag, Berlin, 1995).
- [18] W. Forysiak, J.V. Moloney, and R.G. Harrison, *Physica D* **53**, 162 (1991).
- [19] B. Krauskopf, G.R. Gray, and D. Lenstra, *Phys. Rev. E* **58**, 7190 (1998).
- [20] P. Cvitanovic, *Universality in Chaos: A Reprint Selection* (Adam Hilger, Bristol, 1984).
- [21] Y. Pomeau, and P. Manneville, *Commun. Math. Phys.* **74**, 189 (1980).
- [22] S. Ostlund, D. Rand, J. Sethna, and E. Siggia, *Physica D* **8**, 303 (1983).
- [23] C. Grebogi, E. Ott, and J.A. Yorke, *Phys. Rev. Lett.* **48**, 1507 (1982).
- [24] C. Grebogi and E. Ott, *Physica D* **7**, 181 (1983).
- [25] D. Dangoisse, P. Glorieux, and D. Hennequin, *Phys. Rev. Lett.* **57**, 2657 (1986).
- [26] J.R. Tredicce, F.T. Arecchi, G.L. Lippi, and G.P. Puccioni, *J. Opt. Soc. Am. B* **2**, 173 (1985).
- [27] D. Lenstra, G.H.M. Tartwijk, W.A. van der Graaf, and P.C. De Jagher, *Proc. SPIE* **2039**, 11 (1993).
- [28] T.B. Simpson, J.M. Liu, A. Gavrielides, V. Kovanis, and P.M. Alsing, *Appl. Phys. Lett.* **64**, 3539 (1994).
- [29] A. Hohl and A. Gavrielides, *Phys. Rev. Lett.* **82**, 1148 (1999).
- [30] S. Wieczorek, B. Krauskopf, and Daan Lenstra, *Opt. Lett.* **26**, 816 (2001).
- [31] H. Broer, C. Simo, and J.C. Tatjer, *Nonlinearity* **11**, 667 (1998).

- [32] Yu. Ilyashenko and Li Weigu, *Nonlocal Bifurcations*, Vol. 66 of Mathematical Surveys and Monographs (American Mathematical Society, Providence, RI, 1999).
- [33] E. Doedel, T. Fairgrieve, B. Sandstede, A. Champneys, Yu. Kuznetsov, and X. Wang, computer code *AUTO 97* (<http://indy.cs.concordia.ca/auto/main.html>).
- [34] A. Back, J. Guckenheimer, M.R. Myers, F.J. Wicklin, and P.A. Worfolk, *Not. Am. Math. Soc.* **39**, 303 (1992).
- [35] B. Krauskopf and H.M. Osinga, *J. Comput. Phys.* **146**, 404 (1998).
- [36] B. Krauskopf and H. M. Osinga, in *Numerical Methods for Bifurcation Problems and Large-Scale Dynamical Systems*, Vol. 119 of IMA Volumes in Mathematics and its Applications, edited by E.J. Doedel and L.S. Tuckerman (Springer-Verlag, Berlin, 2000), pp. 199–208.
- [37] S. Wiggins, *Introduction to Applied Nonlinear Dynamical Systems and Chaos* (Springer-Verlag, New York, 1990).